Available online at www.sciencedirect.com

ScienceDirect

Procedia Engineering 79 (2014) 194 – 203

Procedia Engineering

www.elsevier.com/locate/procedia

37th National Conference on Theoretical and Applied Mechanics (37th NCTAM 2013) & The 1st International Conference on Mechanics (1st ICM)

Hole/Crack Identification in Circular Piezoelectric Plates

Yen-Chu Liang[a]* and Yun-Ping Sun[b]

[a]*Department of Aeronautics and Astronautics, Chinese Air Force Academy, GangShan 820, Taiwan*
[b]*Department of Mechanical Engineering, Cheng Shiu University, Kaohsiung 83347, Taiwan*

Abstract

The piezoelectric material generates an electric field when it is deformed by an external force. On account of this electro-mechanical coupling, piezoelectric material plays an important role in the development of sensors as well as actuators. The governing equations of electro-mechanical characteristics are expressed by extended Stroh formalism. The boundary element method is applied to solve the finite domain problem in which the Green function derived according to boundary conditions is embedded. The essential nonlinear identification problem is solved by using the multiple loading modes and stepwise optimization to search for the global minimum solution. This paper successfully identifies the hole/crack size, location, and orientation in finite circular piezoelectric plates by using the strain/electric field data, stress/electric displacement data, or displacement/electric charge data from static loadings. The numerical results that confirm the effectiveness of the proposed method for hole/crack identification in circular piezoelectric plates are presented in details.

Selection and peer-review under responsibility of the National Tsing Hua University, Department of Power Mechanical Engineering

Keywords: Piezoelectric Materials; Hole; Crack; Identification; Plate.

Nomenclature

a	semi-major axis of elliptical hole (m)
$\boldsymbol{a}_\alpha^*$, $\boldsymbol{b}_\alpha^*$	eigenvectors
b	semi-minor axis of elliptical hole (m)

* Corresponding author. Tel.: 886-7-6268881e105.
E-mail address: agliang@cc.cafa.edu.tw

Selection and peer-review under responsibility of the National Tsing Hua University, Department of Power Mechanical Engineering
doi:10.1016/j.proeng.2014.06.331

u_k	displacement (m)
u_i^{kM}	displacement/electrical loading (charge)
C_{ijks}	modulus of elasticity (*Pa*)
D_j	electrical displacement (*Coul/m*^{2} or *Nt/(mVolt)*)
E_j	electrical field (*Nt/coul* or *Volt/m*)
F_M	penalty function for nonlinear optimization
$f_\alpha^*(z_\alpha^*)$	holomorphic functions of complex variables z_α^*
g_l^{kM}	constraints during nonlinear optimization
p_α^*	eigenvalues
$\hat{p}^*$	concentrated loading/charge
R_1	radial coordinate of elliptical hole/crack center in polar coordinates (m)
R_C	radius of circular plate (m)
$\hat{t}_m^*$	traction
$\hat{x}^*$	coordinates of point
σ_{ij}	stress (*Pa*)
σ_{ij}^{kM}	stress/electrical displacement
θ	orientation of hole/crack (rad)
e_{kij}	piezoelectric stress tensor (*Coul/m*^{2} or *Nt/(mVolt)*)
Θ_l	transverse coordinate of elliptical hole/crack center in polar coordinates (rad)
κ_{ik}	permittivity tensor (*Coul*^{2}*/(m*^{2}*Nt)* or *Nt/Volt*^{2})
ε_{ij}^{kM}	strain/electrical field
ϕ_i	stress functions

1. Introduction

In aerospace and mechanical industries the increasing demand to efficiently identify the size, location and orientation of the defect challenges researchers. There are dynamic and static methods to deal with the defect identification. One of the dynamic methods is based on the variation of vibration frequency due to the existence of defects, for example, the non-destructive inspection (NDI) technology to detect the change of natural frequency with the existence of crack or hole by using ultrasonic inspection. The natural frequency varies with the crack depth and location [1,2]. Chen et al. conducted experiment in cantilever beams to detect the crack size and position according to the first three natural frequencies [3]. They reported that the error of size identification was 4% and the error of location identification was 2%. The accuracy of location identification was better than that of size identification. Karthikeyan and Tiwari carried out an experimental investigation to establish an identification procedure for the detection, localization, and sizing of an open flaw in a beam based on forced response measurements [4]. They successfully identified the location and size of the flaw according to the natural frequency variation of the stiffness matrix. The static method is to use the static information, such as stress, strain, and deflection or displacement to identify hole and crack in structures. The vehicles, airplanes and ships in service are subject to many kinds of loading. It is convenient to monitor and gather the static data of critical structures. Researchers found that the measured static data provided a lot of information that could be used to identify the hole and crack effectively [5-9]. Caddemi and Morassi explored the crack identification for elastic beams by static measurement. The crack/hole identifications for composite structures were studied by several researchers in refs [6-9]. If the strains or displacements are not enough sensitive to the size and location of crack in the plate under the static loading, it makes a formidable problem for the crack/hole identification from static data. Hwu and Liang successfully solved the problem by using the multiple loading modes and stepwise optimization. The results of Hwu and Liang's method on hole/crack identification are accurate and stable in the anisotropic composite laminate [6,7]. In this paper the method is extended to the piezoelectric material.

Piezoelectric materials have a wide variety of applications in actuators and sensors because of their coupled electro-mechanical nature. However, their brittleness makes them sensitive to defects like cracks, holes or other type of imperfections. The defects might be owing to improper manufacture and increase or develop during service and

finally result in an irretrievable damage to the system. In general operation, the structural devices are vulnerable to different directional forces, such as the mode one, mode two, and mode three types of forces. The main idea underlying the multiple loading modes and stepwise optimization is to use the static data from different mode type of forces to improve the performance of hole/crack identification in circular piezoelectric plates. The organization of this paper is as follows. Section 2 presents the electro-mechanical formulation of piezoelectric material and the Green functions for the boundary element method to solve the finite domain problems. Section 3 describes the method of multiple loading modes and stepwise optimization using static data to identify hole/crack. Section 4 presents numerical results that confirm the effectiveness of the proposed method for hole and crack identification in finite circular piezoelectric plates. Section 5 concludes the paper.

2. Electro-mechanical Formulation

For an anisotropic linear piezoelectric medium, the constitutive law may be written as

$$\begin{aligned} \sigma_{ij} &= C_{ijks} u_{k,s} - e_{kij} E_k \\ D_i &= e_{iks} u_{k,s} + \kappa_{ik} E_k \end{aligned} \tag{1}$$

where the parameters and the corresponding unit are stress σ_{ij} (unit:*Pa*), displacement u_k (unit:*m*), elasticity tensor C_{ijks} (unit:*Pa*), electrical field E_k (unit: *Nt/coul* or *Volt/m*), electrical displacement D_i (unit: $Coul/m^2$ or *Nt/(mVolt)*), piezoelectric stress tensor e_{iks} (unit: same as D_i), permittivity tensor κ_{ik} (unit: $Coul^2/(m^2 Nt)$ or $Nt/Volt^2$). Because of the full symmetry conditions of the elasticity tensor C_{ijks}, the piezoelectric stress tensor e_{kij} and the permittivity tensor κ_{ik} also satisfy the full symmetry conditions. The governing equations for the mechanical equilibrium and no free charge condition can be expressed by

$$\sigma_{ij,j} = 0, \quad D_{i,i} = 0 \tag{2}$$

An extended version of Stroh formalism [10] satisfying equations (1) and (2) has been derived by Kuo and Barnett [11] as

$$\begin{aligned} \mathrm{u}^* &= \begin{bmatrix} u_1 & u_2 & u_3 & u_4 \end{bmatrix}^T = \mathrm{A}^* \mathrm{f}^*(\mathrm{z}^*) + \overline{\mathrm{A}^* \mathrm{f}^*(\mathrm{z}^*)} \\ \varphi^* &= \begin{bmatrix} \phi_1 & \phi_2 & \phi_3 & \phi_4 \end{bmatrix}^T = \mathrm{B}^* \mathrm{f}^*(\mathrm{z}^*) + \overline{\mathrm{B}^* \mathrm{f}^*(\mathrm{z}^*)} \end{aligned} \tag{3a}$$

where

$$\begin{aligned} &\mathrm{A}^* = \begin{bmatrix} a_1^* & a_2^* & a_3^* & a_4^* \end{bmatrix}, \ \mathrm{B}^* = \begin{bmatrix} b_1^* & b_2^* & b_3^* & b_4^* \end{bmatrix}, \\ &\mathrm{f}^*(\mathrm{z}^*) = \begin{bmatrix} f_1^*(z_1^*) & f_2^*(z_2^*) & f_3^*(z_3^*) & f_4^*(z_4^*) \end{bmatrix}^T, \\ &z_\alpha^* = x_1 + p_\alpha^* x_2, \qquad \alpha = 1,2,3,4. \end{aligned} \tag{3b}$$

u^* and φ^* are 4×1 column vectors. The first three components of u^* are displacements denoted by u_1, u_2, u_3 and the first three components of φ^* are stress functions ϕ_1, ϕ_2, ϕ_3. The last components of u^* and φ^* are expressed as

$$u_{4,i}^* = -E_i \qquad i = 1,2; \ \ \phi_{4,1}^* = D_2 \qquad \phi_{4,2}^* = -D_1. \tag{4}$$

$f_\alpha^*(z_\alpha^*), \alpha = 1,2,3,4$, are four holomorphic functions of complex variables z_α^* , which are determined by the boundary conditions set for each particular problems. The material eigenvalues p_α^* and eigenvectors $\boldsymbol{a}_\alpha^*$, $\boldsymbol{b}_\alpha^*$ are determined by the following eigenrelations

$$\mathrm{N}^*\varsigma^* = p^*\varsigma^*$$
$$\mathrm{N}^* = \begin{bmatrix} \mathrm{N}_1^* & \mathrm{N}_2^* \\ \mathrm{N}_3^* & \mathrm{N}_1^{*\mathrm{T}} \end{bmatrix} \qquad \varsigma^* = \begin{bmatrix} \boldsymbol{a}^* \\ \boldsymbol{b}^* \end{bmatrix} \tag{5}$$

where N^* are the compositions of the material properties. The detailed formulations of N^* can be found in [13]. From a similar derivation in elasticity [12], the infinite anisotropic piezoelectric plate containing an elliptic hole subject to a concentrated loading/charge $\hat{p}^*$ applied at point $\hat{x}^* = (\hat{x}_1, \hat{x}_2)$ is shown in Fig. 1. The boundary conditions are

$$\hat{\mathrm{t}}_\mathrm{m}^* = 0 \qquad \text{along the hole surface}$$
$$\int_\mathrm{C} \mathrm{d}\phi^* = \hat{\boldsymbol{p}}^* \tag{6}$$

where C is any closed curve enclosing the point $\hat{x}^*$. The analytical solutions are:

$$\boldsymbol{f}^*(z^*) = \frac{1}{2\pi i}\left\langle \log(\varsigma_\alpha^* - \xi_\alpha^*)\right\rangle \mathrm{A}^{*\mathrm{T}}\boldsymbol{p}^* + \sum_{k=1}^{4}\frac{1}{2\pi i}\left\langle \log(\varsigma_\alpha^{*-1} - \overline{\xi_k^*})\right\rangle \mathrm{B}^{*-1}\overline{\mathrm{B}^*}\boldsymbol{I}_k\overline{\boldsymbol{A}^{*\boldsymbol{T}}\boldsymbol{p}^*}$$
$$\varsigma_\alpha^* = \frac{z_\alpha^* + \sqrt{z_\alpha^{*2} - a^2 - p_\alpha^{*2}b^2}}{a - ip_\alpha^* b} \tag{7}$$

where a and b are semi-major axis and semi-minor axis shown in Fig. 1. I_k is the 4×4 diagonal matrix with 1 on the k^{th} main diagonal and zeros elsewhere. The analytical solutions of straight crack problems are the same as equation (7) by letting b approach zero.

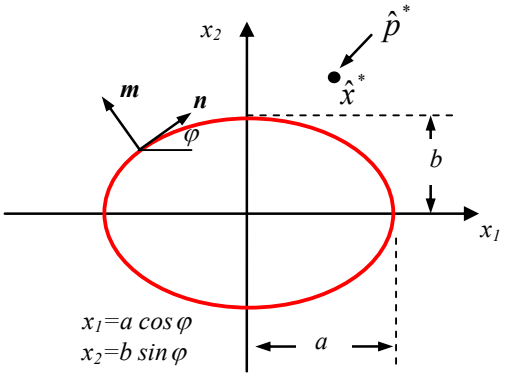

Fig. 1. Infinite plate with elliptical hole subjected to an arbitrary loading/charge.

To solve the finite domain problems, the boundary element method as an approximate numerical technique has been successfully applied for a wide variety of areas. According to the former research [13], it is a feasible approach to solving the finite piezoelectric material problem by the numerical program of boundary element method in which the analytical solution equation (7) was embedded. The forward analysis of the effect of variations of size, location, and orientation of crack/hole on strains/electrical fields, stresses/electrical displacement or displacement/electrical load in circular plates is similar to that in square plates. Because the shape of the plate is not square, the pure loading

mode as depicted in Fig. 2 is hardly to be defined in a circular plate. Therefore, the multiple loading modes of a circular plate are defined to be three types of mixed loading modes as follows.

- mode I : load along the radius direction R of the circular plate which is the combination of the loading direction x_1 and x_2 in Cartesian coordinate system,
- mode II: load in the anti-plane direction,
- mode III: electrical displacement along the radius direction R .

The definition of the size (a, b), location (R_1, Θ_1) and orientation (θ) of crack/hole in a circular plate is shown in Fig. 3. Note that the magnitude of the measured variables to be used to identify hole/crack in piezoelectric materials such as strains, displacements, electric charges, and electric displacements are usually very small. It is important in practice that the measured variables in each loading mode must be carefully selected to keep good sensitivity.

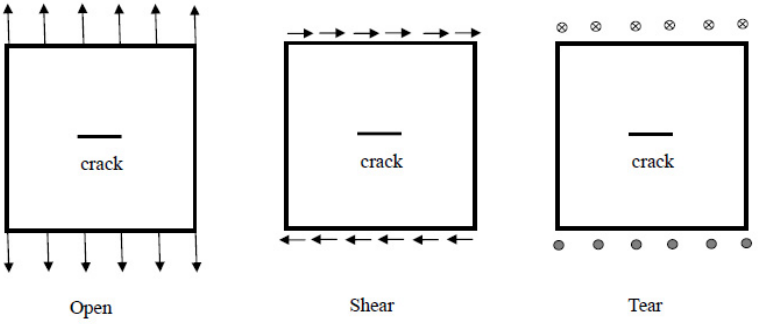

Fig. 2. Three typical types of loading modes for crack in the plate.

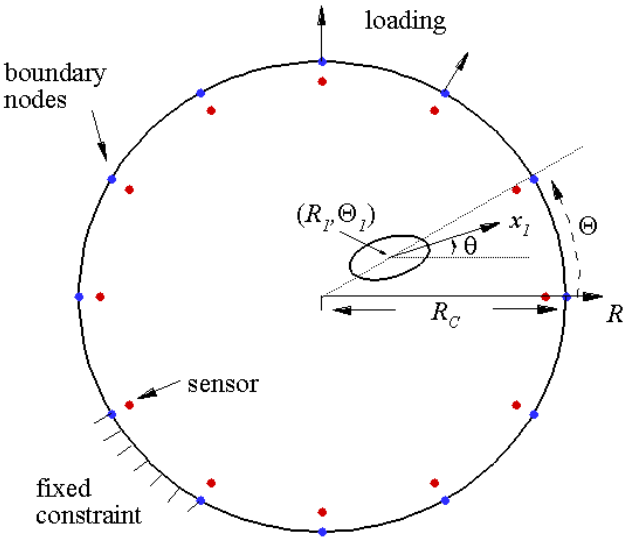

Fig. 3. Location (R_1,Θ_1) and orientation θ of elliptical hole, sensors arrangement and boundary conditions around the circular plate.

3. Hole and Crack Identifications

The measured variables used for hole/crack identification are strain/electrical field ε_{ij}, stress/electrical displacement σ_{ij}, displacement/electrical loading (charge) u_i. Assume that they are functions of hole/crack properties and location of sensors and can be expressed as

$$\begin{aligned} \varepsilon_{ij}^{kM} &= \varepsilon_{ij}(R_1, \Theta_1, \theta, a, b, s_k)_M \\ \sigma_{ij}^{kM} &= \sigma_{ij}(R_1, \Theta_1, \theta, a, b, s_k)_M \\ u_i^{kM} &= u_i(R_1, \Theta_1, \theta, a, b, s_k)_M \end{aligned} \tag{8}$$

where R_1, Θ_1, θ, a and b are hole/crack properties, s_k is sensor number to denote the measured location, M is the type of mixed loading mode. Nonlinear optimization [14] is applied by using different measured variables in equation (8) with different type of mixed loading modes, different sensor positions, and different hole/crack properties such as size a, b, orientation θ, and position R_1, Θ_1.

At first, a set of star values of measured variables including ε_{ij}^{kM*}, σ_{ij}^{kM*}, and u_i^{kM*} from a known hole/crack target in which the target size a^* and b^*, target orientation θ^*, and target position R_1^*, Θ_1^* are specified. The initial guesses of design variables are random. We search for the target values of design variables by minimizing the penalty function that represents the differences between the estimated values and star values of measured variables. From the experiences in hole/crack identification for elastic square plates [6], the insensitivity of static strains to hole/crack geometry and location resulting from the local effect of hole/crack identification problems may be overcome by introducing the multiple loading modes approach. The approach is described as follows. We start an identification for hole/crack by a given loading mode condition until the penalty function cannot be reduced further. Then switch to another loading mode. Let the results of the previous identification be the initial guess of the next identification and carry on the identification again. Repeat this process until the convergence criterion is satisfied. According to this concept, a multistep nonlinear optimization is designed in the following.

Minimize:

$$F_M = \sum_{k=1}^{n_s} \sum_{l=1}^{n_m} (H_l^{kM} / H_l^{kM*} - 1)^2 \tag{9a}$$

Subject to:

$$g_l^{kM} = \left| H_l^{kM} / H_l^{kM*} - 1 \right| - e_M < 0, \begin{cases} k = 1, 2, ..., n_s \\ l = 1, 2, ..., n_m \end{cases} \tag{9b}$$

$$0 < R_1 < R_C \text{ , } 0 < \Theta_1 < 2\pi \text{ , } 0 < \theta < \pi, \; 0 < a < R_C / 3, \; 0 < b < R_C / 3 \tag{9c}$$

where H_l^{kM} represents the measured variables in equation (8) for each loading mode M; k is the index of sensors and total number of sensors is n_s; l is the index of measured variables and total number of measured variables is n_m; e_M is the tolerance of error for loading mode M; and R_C is the radius of piezoelectric circular plate. Note that the measured variables are different when the loading mode changes. The static measured variables H_l^{kM} for each loading mode are:

(1) Loading mode I (M=1) : strain $\varepsilon_{RR}, \varepsilon_{R\Theta}, \varepsilon_{\Theta\Theta}$, ($l$=1~3), stress $\sigma_{RR}, \sigma_{R\Theta}, \sigma_{\Theta\Theta}$, ($l$=4~6) and displacement u_R, u_Θ. (l=7,8).

(2) Loading mode II (M=2) : strain $\varepsilon_{Rz}, \varepsilon_{\Theta z}, \varepsilon_{zz}$, ($l$=1~3), stress $\sigma_{Rz}, \sigma_{\Theta z}, \sigma_{zz}$, ($l$=4~6) and displacement u_Z. (l=7).

(3) Loading mode III (M=3) : electric field E_R, E_Θ, E_z, (l=1~3), electric displacement D_R, D_Θ, D_z, (l=4~6) and electric charge q(=u_4, l=7).

In order to obtain a good convergence, the tolerance of error should not be set too small at the beginning identification process. We gradually decrease the tolerance of error in the successive identification process of different loading modes. When the constraint conditions are satisfied and the data of measured variables approach star values, the penalty function will decrease continuously. The details of numerical results of hole/crack identification are described in the next section.

4. Numerical Results

We use the piezoelectric material PZT4 in the following numerical examples and the material properties are summarized in Table 1. In Fig. 3, the loading stimuli applied in the boundary nodes are stress ($1Pa$), or electric displacement (1000 Coul/m^2). The optimization methods are feasible direction method and golden section method [14].

Table 1. Material properties of piezoelectric material PZT4.

$S_{11}=1.09\times10^{-11}$ m^2/Nt	$S_{33}/S_{11}=0.725$	$g_{33}=2.61\times10^{-2}$ Volt · m/Nt	$\varepsilon_{11}=8.697\times10^{7}$ Volt^2/Nt
$S_{12}/S_{11}=-0.497$	$S_{44}/S_{11}=1.771$	$g_{13}/g_{33}=-0.425$	$\varepsilon_{33}/\varepsilon_{11}=0.881$
$S_{13}/S_{11}=-0.193$	$S_{66}/S_{11}=2.994$	$g_{15}/g_{33}=1.510$	

4.1. Identification of crack size only

In order to test the performance of the numerical program, we let b=0 and fix the position and orientation of crack at first. The crack size a is the only one variable to be identified. The measured data are stresses $(\sigma_{RR},\sigma_{R\Theta},\sigma_{\Theta\Theta})$ and electric displacement (D_R,D_Θ,D_z). There are 12 equally spaced sensors s_k (k=1~12) located at $R_C/10$ away from the boundary of circular plate. The loading stimulus is stress along the R direction in the upper-right boundary nodes shown in Fig. 3. The fixed constraints are set in the lower-left boundary nodes shown in Fig. 3. There is a horizontal crack in the center of the plate to be identified. The crack length is $2a$=4cm. The diameter of the circular plate is 10cm. The identified results are shown in Table 2. The tolerance of error e_M is set to 0.001 and radius of circular plate is 5 cm. After 8 iterations, the final identified result of crack size is 1.9964 cm and the penalty function decrease to $F_M=3.62\times10^{-4}$. Apparently it is successful to identify one variable, crack size, only. As the number of identified variables increases, the problem becomes more challenging. The multiple loading modes method is applied to inject new energy to solve the identification problem.

Table 2. Size identification of horizontal crack.

		a(cm)	Penalty function F_M
Target value		2	0.
Initial guess		0.2	0.34198
Identified procedures	Iteration 1	0.3001	0.30651
	Iteration 2	0.6178	0.22239
	Iteration 3	1.2938	9.8122172E-02
	Iteration 4	2.3877	4.6605524E-02
	Iteration 5	4.1576	0.2247717
	Iteration 6	2.1885	2.3105575E-02
	Iteration 7	2.2104	2.5721302E-02
	Iteration 8	1.9964	3.6152947E-04
	error	0.18%	$F_M<e_M$

4.2. Identification of hole

In this numerical example for hole identification, the radius of plate is set to be 6 cm. Because we are going to use multiple loading modes method, the magnitude of different type of measured variables has to be considered

carefully. For piezoelectric materials in comparison with the stress the electric displacement and strain is usually very small. In order to obtain a better sensitivity, we use the normalized form $H_l^{kM}/H_l^{kM*}-1$ instead of $H_l^{kM}-H_l^{kM*}$ as the penalty function in Equation (9). The location, size, and orientation of target hole are (R_1 ,Θ_1)=(2, 0.524), (a,b)=(1, 0.5), and θ=0.262. The initial guess are (R_1 ,Θ_1)=(0,0), a=b=*1.5*, and θ=0. On the basis of nonlinear optimization using multiple loading modes, the optimal identification results of each loading mode are used as an initial guess of the next optimization for a different loading mode until the final results satisfy the convergence criterion. Let us compare the results of hole identification obtained by using the data of different type of measured variables in Table 3. It indicates that the best identification is using the strain/electric filed data, the second is using the stress/electric displacement data, and the third is using the displacement/electric charge data. The sequence of applied loading mode, tolerance of error, and iteration number of identification by using three types of measured data such as strain/electric filed, stress/electric displacement, and displacement/electric charge is given in the following three paragraphs.

Identification from strain/electric filed data: (1) mode I, e_M=0.5, 36 iterations, (2) mode II, e_M=0.1, 28 iterations, (3) mode III, e_M=0.05, 42 iterations, (4) mode I, e_M=0.05, 58 iterations, (5) mode III, e_M=0.01, 44 iterations, (6) mode II, e_M=0.01, 61 iterations, (7) mode I, e_M=0.001, 73 iterations. The detailed identification results are presented in Table 4.

Identification from stress/electric displacement data: (1) mode I, e_M=0.5, 23 iterations, (2) mode II, e_M=0.1, 46 iterations, (3) mode III, e_M=0.05, 57 iterations, (4) mode I, e_M=0.05, 62 iterations, (5) mode III, e_M=0.01, 71 iterations, (6) mode II, e_M=0.01, 58 iterations.

Identification from displacement/electric charge data: (1) mode I, e_M=0.5, 26 iterations, (2) mode II, e_M=0.1, 31 iterations, (3) mode III, e_M=0.05, 37 iterations, (4) mode I, e_M=0.05, 49 iterations, (5) mode III, e_M=0.01, 53 iterations, (6) mode II, e_M=0.01, 49 iterations, (7) mode I, e_M=0.005, 58 iterations, (8) mode III, e_M=0.001, 82 iterations, (9) mode II, e_M=0.001, 63 iterations, (10) mode I, e_M=0.001, 87 iterations.

Although we use 10 loading modes and reduce the tolerance of error to 0.001, the identification results by using displacement/electric charge data are still not quite satisfactory. It is possible that the initial guess, the sequence of loading modes, and even the magnitude of tolerance error affect the accuracy and efficiency of hole/crack identification. We recognize that it is difficult to find a golden rule to further improve the identification performance. However, the proposed multiple loading mode method effectively achieves a stable and acceptable identification results. Note that the number of sensors is 12 in Table 3 and 4.

Another interesting topic would be to examine the effect of using different number of sensors on identification accuracy. The sensors are equally spaced on the boundary of the circular plate. We use the same target values and initial guess described above in this subsection to carry out hole identification. Fig. 4(a) shows the identified results in comparison with using 6, 8, and 12 sensors. It suggests that the more sensors will result in the better identification. The blue solid line represents the target hole. The red square symbols on the boundary mark the locations of 6 sensors, the black circular and red square symbols mark the locations of 12 sensors, and the locations of 8 sensors are not marked for simplicity. The dotted line represents the identification results from 6 sensors, the dash-dotted line represents that from 8 sensors, and the dashed line represents that from 12 sensors. All identification results are satisfactory that clearly indicate the size, location, and orientation of target hole.

Table 3. Results of hole identifications using different type of measured variables.

		R_1(cm)	Θ_1(rad)	θ(rad)	a(cm)	b(cm)
Target value		2	0.524	0.262	1	0.5
Initial guess		0	0	0	1.5	1.5
strain/electrical field	Identified results	2.08	0.588	0.287	1.01	0.51
	Error	4.0%	12.3%	9.5%	1.2%	2.5%
stress/electrical displacement	Identified results	2.19	0.604	0.282	1.07	0.54
	Error	9.4%	15.2%	7.6%	6.7%	7.6%
displacement/ electrical charge	Identified results	1.78	0.643	0.315	1.14	0.60
	Error	10.8%	22.8%	20.3%	14.1%	20.3%

Table 4. Results of hole identification using strain/electric field data.

	R_1(cm)	Θ_1(rad)	θ(rad)	a(cm)	b(cm)
Target value	2	0.524	0.262	1	0.5
Initial guess	0	0	0	1.5	1.5
Loading mode I e_M=0.5, 36 iterations	1.52	0.478	0.313	0.67	0.62
Loading mode II e_M=0.1, 28 iterations	1.43	0.421	0.398	0.72	0.63
Loading mode III e_M=0.05, 42 iterations	1.81	0.545	0.326	0.82	0.59
Loading mode I e_M=0.05, 58 iterations	1.87	0.582	0.355	0.86	0.57
Loading mode III e_M=0.01, 44 iterations	1.93	0.538	0.305	1.17	0.56
Loading mode II e_M=0.01, 61 iterations	1.88	0.482	0.318	0.93	0.55
Loading mode I e_M=0.001, 73 iterations	2.08	0.588	0.287	1.01	0.51

4.3. Identification of Crack

The design variables for crack identification are location (R_1 ,Θ_1), orientation θ and size a. Let the radius of plate R_C be 5 cm, the size of the target crack be one fifth of R_C, i.e., a=1cm, the location of the target crack be on the lower left side of the circular plate shown in Fig. 4(b), the orientation of the target crack be 15^o. Because of the local (regional) characteristics of crack, the sensitivity to measured variables of crack identification is not as high as that of the hole identification. As a result, it requires more loops of multiple loading modes to perform the nonlinear optimization for crack identification. The results of crack identification are shown in Table 5 and the identified crack trajectory is depicted in Fig. 4(b). Although the maximum percentage error is crack size a which is 19.2% in Table 5, it is noted that Id10 and Id11 are very close to the target crack as shown in Fig. 4(b). Sometimes the identified results will be trapped into the local minimum. It is very important to use the multiple loading modes to kick the identification result out of the local minimum and keep searching for the global minimum till the strict error tolerance is satisfied.

Table 5. Results of crack identifications.

		R_1(cm)	Θ_1(rad)	θ(rad)	a(cm)
Target value		3	3.927	0.262	1
Initial guess		0	0	0	2
Id1	Loading mode I e_M=0.5, 27 iterations	5.39	4.974	0.179	1.67
Id2	Loading mode II e_M=0.1, 41 iterations	4.61	3.054	0.105	1.52
Id3	Loading mode III e_M=0.05, 32 iterations	4.68	3.107	0.611	1.43
Id4	Loading mode I e_M=0.05, 45 iterations	4.29	0.262	0.733	1.22
Id5	Loading mode II e_M=0.05, 51 iterations	3.78	5.201	0.401	1.23
Id6	Loading mode III e_M=0.01, 29 iterations	3.51	2.356	0.372	1.48
Id7	Loading mode II e_M=0.01, 47 iterations	3.27	0.820	0.337	1.37
Id8	Loading mode I e_M=0.01, 83 iterations	3.42	4.451	0.355	1.21
Id9	Loading mode III e_M=0.005, 53 iterations	3.30	4.189	0.314	1.31
Id10	Loading mode I e_M=0.001, 117 iterations	3.49	4.102	0.231	1.13
Id11	Loading mode II e_M=0.001, 79 iterations	3.35	4.643	0.283	1.19
Error		11.5%	18.2%	8.2%	19.2%

5. Conclusions

This paper presents an effective hole/crack identification method for a finite circular piezoelectric plate by using the static deformation data such as strain/electrical field, stress/electrical displacement, and displacement/electrical

charge. The essence of the identification method is a multi-step nonlinear optimization process applying the multiple loading modes to prevent the local minimum solution. According to the numerical results, when the hole/crack size is one sixth or one fifth of the radius of piezoelectric plate and 12 sensors is used, the maximum percentage error for hole identification is location error which is under 13%, and the maximum percentage error for crack identification is size error which is under 20%. It indicates that not only the hole/crack size but also the location and orientation can be satisfactorily identified.

Acknowledgements

The authors would like to thank the National Science Council, Taiwan, R.O.C.,for financial support under grant No: NSC 99-2221-E-013-001.

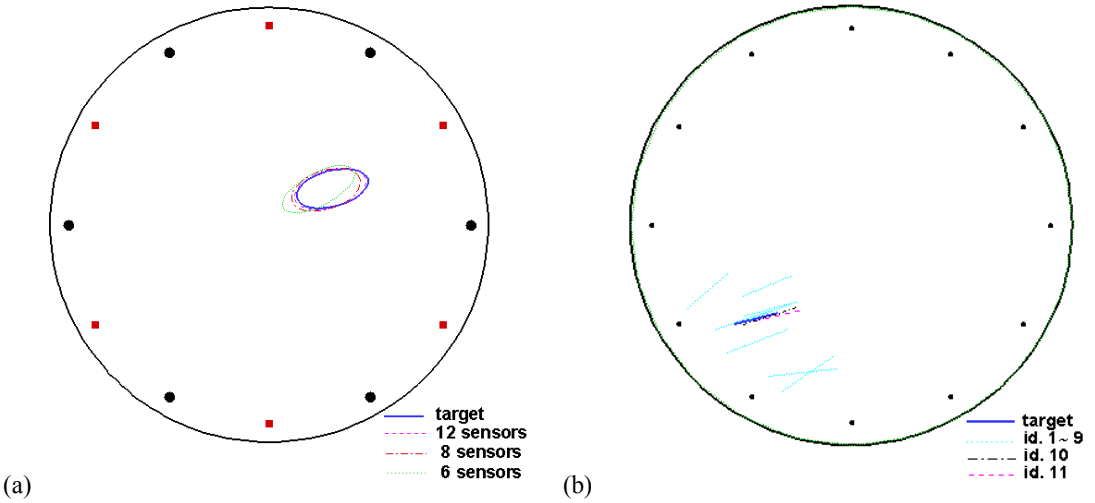

Fig. 4. (a) Results of hole identification in comparison with different number of sensors, (b) Results of crack identification.

References

[1] N. Khaji, M. Shafiei, M. Jalalpour, Closed-form solutions for crack detection problem of Timoshenko beams with various boundary conditions, Int. J. Mech. Sci. 51 (2009) 667-681.
[2] J. Lee, Identification of multiple cracks in a beam using vibration amplitudes, J. Sound and Vibration 326 (2009) 205-212.
[3] X.F. Chen, Z.J. He, J.W. Xiang, Experiments on crack identification in cantilever beams, Experimental Mech. 45 (2005) 295-300.
[4] M. Karthikeyan, R. Tiwari, Detection, localization, and sizing of a structural flaw in a beam based on forced response measurements – An experimental investigation, Mechanism and Machine Theory 45 (2010) 584-600.
[5] S. Caddemi, A. Morassi, Crack detection in elastic beams by static measurements, Int. J. Solids and Structures 44 (2007) 5301-5315.
[6] C. Hwu, Y.C. Liang, Hole/Crack Identification by Static Strains from Multiple Loading Modes, AIAA Journal 39 (2001) 315-324.
[7] Y.C. Liang, C. Hwu, On-line Identification of Holes/Cracks in Composite Structures, Smart Materials and Structures 10 (2001) 599-609.
[8] G. Rus, S.Y. Lee, R. Gallego, Defect identification in laminated composite structures by BEM from incomplete static data, Int. J. of Solids and Structures 42 (2005) 1743-1758.
[9] L.H. Yam, Y.Y. Li, W.O. Wong, Sensitivity studies of parameters for damage detection of plate-like structures using static and dynamic approaches, Eng. Structures 24 (2002) 1465-1475.
[10] A.N. Stroh, Dislocations and Cracks in Anisotropic Elasticity, Phil. Mag., 7 (1958) 625.
[11] C.M. Kuo, D.M. Barnett, Stress Singularities of Interfacial Cracks in Bonded Piezoelectric Half-Spaces, in: J.J. Wu, TCT Ting, D.M. Barnett (Eds.), Modern Theory of Anisotropic Elasticity and Applications, SIAM, 1991, pp. 33-50.
[12] C. Hwu, W.J. Yen, Green's Functions of Two-Dimensional Anisotropic Plates Containing an Elliptic Hole, Int. J. of Solids Structures, 27 (1991) 1705-1719.
[13] Y.C. Liang, C. Hwu, Electromechanical Analysis of Defects in Piezoelectric Materials, Smart Materials and Structures, 5 (1996) 314-320.
[14] G.N. Vanderplaats, Numerical Optimization Techniques for Engineering Design: With Applications, N.Y.: McGraw-Hill, 1984.